Study of Magnetoconvection Impact on a Coil Cooling by Ferrofluid with a Spectral/Finite-Element Method

Raphael Zanella, Caroline Nore, Frédéric Bouillault, Loic Cappanera, Ignacio Tomas, Xavier Mininger, Jean-Luc Guermond

Study of Magnetoconvection Impact on a Coil Cooling by Ferrofluid with a Spectral / Finite Element Method

Raphaël Zanella[1,2], Caroline Nore[1], Frédéric Bouillault[2], Loic Cappanera[3], Ignacio Tomas[3], Xavier Mininger[2], and Jean-Luc Guermond[3]

[1]LIMSI, CNRS, Univ. Paris-Sud, Université Paris-Saclay, F-91405 Orsay, France
[2]GeePs, UMR 8507 CNRS / CentraleSupelec - Universités UPMC et UPSud, 91192 Gif sur Yvette cedex, France
[3]Department of Mathematics, Texas A&M University, College Station, TX 77843 USA

The benefit of magnetoconvection for transformer cooling by ferrofluid is numerically studied. A code combining spectral and finite element methods is applied on a solenoid system. Magnetostatic, Navier-Stokes and energy equations are solved simultaneously. A vegetable oil seeded with magnetite nanoparticles at a volume fraction of 10 % is considered. The magnetization of the ferrofluid is function of temperature through an approximation of the classical Langevin's law. Magnetic and temperature fields are used to update the magnetic action, modeled by the Kelvin force, on the ferrofluid momentum at each time step. Numerical results for regular oil are consistent with experimental temperature data obtained for pure vegetable oil cooling. Numerical results for ferrofluid show that the magnetoconvection modifies the flow convection pattern and speed. The temperature increase in the coil is consequently reduced by about 9.4 % with ferrofluid cooling.

***Index Terms*—coupled problem, finite element, magnetoconvection, spectral method, transformer cooling.**

I. Introduction

A FERROFLUID is a stable suspension of magnetic nanoparticles in a non magnetic liquid carrier. A magnetic field transfers momentum to the ferrofluid through the nanoparticles. Literature often mentions the Kelvin force model (in N/m^3) to consider this effect [1],

$$\boldsymbol{F} = \mu_0(\boldsymbol{M} \cdot \nabla)\boldsymbol{H}, \quad (1)$$

where $\boldsymbol{M}$ is the magnetization and $\boldsymbol{H}$ the magnetic field.

The dependence of the magnetization with respect to temperature can lead to magnetoconvection when magnetic field and temperature gradients are combined, as it is the case in immersed transformers [2]. If the heat transfer rate is increased because of the nanoparticles, the volume of cooling fluid could be reduced, or mechanical cooling systems avoided. Moreover, instead of conventional mineral oil, the liquid carrier could be substituted by vegetable oil, with higher viscosity but biodegradable and non toxic.

Heat transfer enhancement when using ferrofluid instead of regular oil was pointed out in the work on an immersed coil [3]. Encouraging results on a transformer were obtained in [4] but the ferrofluid magnetization model was temperature independent. The experimental work based on a transformer prototype [5] also showed the benefit of ferrofluid as coolant. In this work, a setup close to that of [3] is simulated with the SFEMaNS code [6], based on spectral and finite element methods. The ferrofluid magnetization follows an approximation of the Langevin's law [7] to include the effects of temperature dependence. Dynamic and symmetry features of the solutions, with or without nanoparticles, are presented and the decrease of the coil temperature with ferrofluid cooling is explained by studying the flow pattern.

In a first step, a simulation without Kelvin force is ran to validate the model against experiments with pure vegetable oil. In a second step, the Kelvin force is added and the numerical results for regular oil and ferrofluid are compared.

Manuscript received April 1, 2015; revised May 15, 2015 and June 1, 2015; accepted July 1, 2015. Date of publication July 10, 2015; date of current version July 31, 2015. Corresponding author: R. Zanella (e-mail: zanella@limsi.fr).

Color versions of one or more of the figures in this paper are available online at http://ieeexplore.ieee.org.

Digital Object Identifier (inserted by IEEE).

II. Experimental and Numerical Setup

A. Experimental Setup

The experiments [8] are based on an electromagnetic system constituted of a triple copper coil crossed by a DC current and immersed in vegetable oil, as presented in Fig. 1. The fluid is a sample of oil produced by the Midel company for transformer cooling. The temperature increase is locally measured at the boundary of the coil and in the fluid until a steady state is reached (typically 10000 s time).

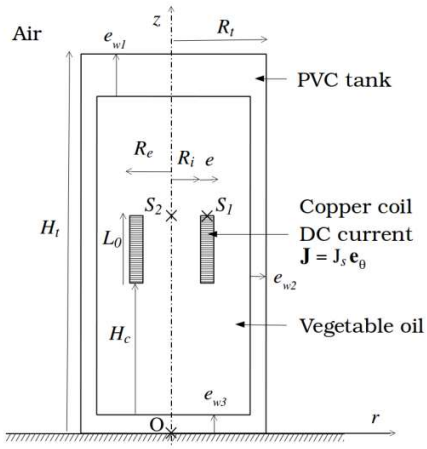

Fig. 1. Experimental setup model. S_1 and S_2 represent the thermal sensors.

The dimensions are: $H_t = 12.5$ cm, $R_t = 2.5$ cm, $R_i = 0.8$ cm, $R_e = 1.175$ cm, $e = 0.375$ cm, $L_0 = 2.1$ cm, $H_c = 3.9$ cm, $e_{w1} = 2$ cm, $e_{w2} = 0.45$ cm, and $e_{w3} = 1$ cm.

The current in each spire, about 8 A, is controlled with a dSPACE setup so that the power dissipated in the coil keeps its initial value of 3.0 W over the period of measurement. The coil electrical resistance decrease due to the heating by Joule effect is thus counterbalanced.

B. Modeling

Regular oil and ferrofluid cases use the same equations, except for the body forces in the momentum equation, as presented hereafter. Quasi-steady regime approximation for electromagnetism is used. Like the regular oil, the ferrofluid is a continuum medium with Newtonian fluid behavior. Boussinesq approximation is used and viscous dissipation is neglected. Regarding the ferrofluid, its magnetization is assumed to be instantaneously aligned with the magnetic field. Finally, the transient term containing the pyromagnetic coefficient in the energy equation of [1] is also neglected.

The magnetostatic equations are

$$\nabla \times \boldsymbol{H} = \boldsymbol{J}, \tag{2}$$

$$\nabla \cdot (\mu \boldsymbol{H}) = 0, \tag{3}$$

where $\boldsymbol{J}$ is the current density (enforced current density $J_s \boldsymbol{e}_\theta$ in the coil, null elsewhere) and μ the magnetic permeability.

The Navier-Stokes equations are

$$\rho \partial_t \boldsymbol{u} + \rho(\boldsymbol{u} \cdot \nabla)\boldsymbol{u} + \nabla p - \eta \Delta \boldsymbol{u} = \alpha(T - T_0)\rho g \boldsymbol{e}_z + \mu_0 M \nabla H, \tag{4}$$

$$\nabla \cdot \boldsymbol{u} = 0, \tag{5}$$

where ρ is the density, $\boldsymbol{u}$ the velocity, p the pressure, η the dynamic viscosity, α the thermal expansion, T the temperature, T_0 the exterior temperature and g the gravity. The first term of the right hand side is the Boussinesq force and the second represents the simplified expression of the Kelvin force in (1), considering that $\boldsymbol{M}$ and $\boldsymbol{H}$ are collinear [1].

The conservation of energy is written as

$$\rho c \partial_t T + \rho c(\boldsymbol{u} \cdot \nabla)T - \nabla \cdot (\lambda \nabla T) = f_T, \tag{6}$$

where c is the heat capacity, λ the thermal conductivity and f_T the heat source, equal to the Joule effect J_s^2/σ_{cl} in the coil and null elsewhere (σ_{cl} is the coil electrical conductivity).

The boundary condition for the magnetic problem is: $\boldsymbol{H} \times \boldsymbol{n} = 0$ on the tank's exterior border. A non-slip boundary condition is enforced: $\boldsymbol{u} = 0$ on the border of the fluid domain. The air convection at the top and the lateral boundaries of the tank is modeled using a Robin boundary condition on temperature:

$$-\lambda \nabla T \cdot \boldsymbol{n} = h(T - T_0), \tag{7}$$

where h is the convection coefficient and $\boldsymbol{n}$ the outer normal vector. The Dirichlet condition $T = T_0$ is enforced on the bottom of the tank, that part of the fluid domain being slightly affected by convection. Initially, $\boldsymbol{u} = 0$, $T = T_0$, and $\boldsymbol{H} = 0$.

The magnetization intensity of the ferrofluid is proportional to the magnetic field intensity:

$$M = \chi(T)H, \tag{8}$$

with χ the susceptibility given by an approximation of the Langevin's law [7]:

$$\chi(T) = \frac{\varphi \mu_0 \pi d^3 M_0^2}{18 k_B (T + 273.15)}. \tag{9}$$

where φ is the volume fraction of magnetic material, d the particle diameter, M_0 the particle magnetization and k_B the Boltzmann constant.

The thermo-physical properties used in each subdomain (coil, fluid, tank) are presented in Table 1.

TABLE I
THERMO-PHYSICAL PROPERTIES

Property	Coil	Fluid	Tank
Density (kg/m^3)	3888	922	1400
Dynamic viscosity (Pa.s)	-	2.9e-2	-
Thermal expansion (/K)	-	7.4e-4	-
Heat capacity (J/K/kg)	622	1970	1000
Thermal conductivity (W/m/K)	0.361	0.166	0.16

The viscosity is set to the value taken at 40 °C, the temperature approximately reached in the experiments. The other fluid properties present reduced variations over the temperature range and are taken at 20 °C.

In the model, the coil represents the copper coil itself and the oil stuck by viscosity between the spires. The properties are homogeneous properties between copper and Midel oil properties, the fraction of copper being approximately 37 %. The density and the heat capacity are obtained using a mix law. The thermal conductivity is given by the analytical law developped by [9].

The temperature in the lab is measured at $T_0 = 18$ °C. The tank / air convection coefficient is chosen in the range given by the literature: $h = 17$ W/m^2/K. The Joule effect and the current density in the coil are calculated to be consistent with the enforced current in the experiment.

A ferrofluid containing magnetite nanoparticules with classical characteristics is considered: $\varphi = 0.1$, $d = 10$ nm and $M_0 = 446$ kA/m. In the magnetostatic equation (4), the magnetic permeability μ is piecewise constant: $\mu_0(1 + \chi(T_0))$ in the ferrofluid and μ_0 elsewhere.

III. THE SFEMANS CODE

A. Numerical method

To investigate the hydrodynamic and thermal regimes of the above experimental set-up, we use our own magneto-hydrodynamics code called SFEMaNS, see [6].

The code uses a hybrid spatial discretization mixing Fourier expansions and finite elements. The method is based on cylindrical coordinates and every field f is solved as a partial Fourier sum relative to the azimuthal direction:

$$f(r,\theta,z) = f_0^c(r,z) + \sum_{m=1}^{m_{max}} f_m^c(r,z)\cos(m\theta) + \sum_{m=1}^{m_{max}} f_m^s(r,z)\sin(m\theta), \tag{10}$$

where m_{max} is the maximum considered mode. The problem can be approximated independently (modulo the computations of nonlinear terms) for each Fourier mode in the meridian plane with Lagrange finite elements. First order elements are used for the pressure while second order elements are used for the temperature and the velocity. For the magnetic part, the algorithm solves the problem using the magnetic field $\boldsymbol{H}$ in the conducting region (after standard elimination of the electric field) and a scalar magnetic potential ($\boldsymbol{H} = \nabla\phi$) in the insulating exterior if needed. The fields in each region are

approximated by using H^1-conforming Lagrange elements, with a technique to enforce $\nabla \cdot (\mu \boldsymbol{H}) = 0$ based on a penalty method. This method has been proved to converge under minimal regularity [10] and has been validated in [11] for example. The coupling across the axisymmetric interfaces where the electric conductivity or the magnetic permeability is discontinuous is done by using an interior penalty method.

SFEMaNS has been thoroughly validated on numerous analytical solutions and against other magneto-hydrodynamics codes [6,12].

B. Validation on a Rayleigh-Bénard convection test case

We study a classical Rayleigh-Bénard convection problem in a cylindrical cavity heated from below and insulated laterally following [13]. Using non-slip boundary conditions on the lateral wall, the motionless conducting state of a cylinder of radius to height aspect ratio of $R/H = 0.75$ becomes unstable above a critical Rayleigh number

$$Ra = \frac{\alpha \Delta T g H^3}{\kappa \nu} = 2590, \tag{11}$$

where ΔT is the characteristic temperature difference, κ the thermal diffusivity and ν the kinematic viscosity, in excellent agreement with [13]. The stationary convection forms a roll corresponding to a $m = 1$ mode which breaks the axisymmetry of the base state (see Fig. 2).

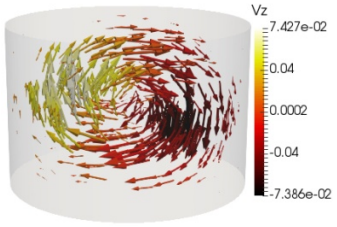

Fig. 2. Rayleigh-Bénard convection roll [13] simulated by SFEMaNS.

IV. Results

A. Comparison with the experiment on pure vegetable oil

The flow and temperature fields are simulated in the experiment case of pure vegetable oil. In (4), the only force is the Boussinesq one and (2) and (3) are not solved.

Computations show that, for the chosen parameters, the steady solution is carried by the mode 0 only, i.e. is axisymmetric. Even initially populated, the other modes vanish and $m_{max} = 0$ in (10) is chosen. The mesh contains 3031 nodes and a time step of 0.02 s is used over $5\text{x}10^5$ iterations (about 11 wall-clock hours using 8 processors on the cluster IBM x3750-M4 from GENCI-IDRIS).

The numerical solution reaches a steady regime in about 10000 s, a time consistent with the experimental observation. Fig. 3 presents the time evolution of the kinetic energy:

$$E_k(t) = \int_{\Omega_f} \frac{1}{2} \rho u^2(\boldsymbol{x}, t) d\boldsymbol{x}, \tag{12}$$

where Ω_f is the fluid domain, and the spatial quadratic mean of the temperature increment:

$$\overline{T - T_0}(t) = \sqrt{\frac{1}{V} \int_{\Omega} (T - T_0)^2(\boldsymbol{x}, t) d\boldsymbol{x}}, \tag{13}$$

where Ω is the whole domain and V its volume. These global quantities show that velocity and temperature fields eventually reach a stationary state.

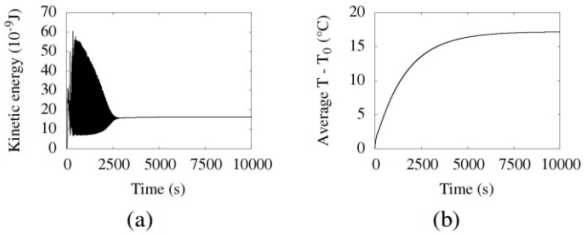

Fig. 3. Time evolution of the kinetic energy (a) and the spatial quadratic mean of the temperature increment $T - T_0$ in the regular oil case.

The numerical results for temperature are in good agreement with the experimental data, as shown in Fig. 4.

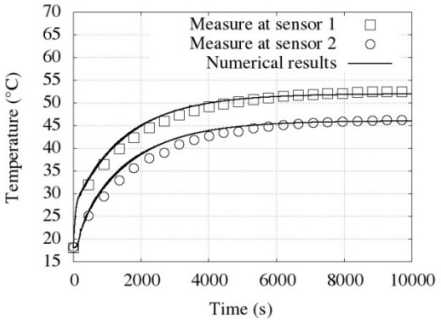

Fig. 4. Comparison of the temperature increase obtained experimentally and numerically in the pure vegetable oil case. Experimental data from [8].

B. Numerical results on magnetoconvection

The code is here used to assess the effect of the magnetoconvection when the vegetable oil is replaced by ferrofluid. Both Boussinesq and Kelvin forces create momentum in (4). In these simulations, the regular oil and the ferrofluid have the same thermo-physical properties to highlight the Kelvin force effect.

Again, the simulation is run with $m_{max} = 0$. The same numerical setup (mesh, time step, processors) leads to a completed computation in about 16 wall-clock hours.

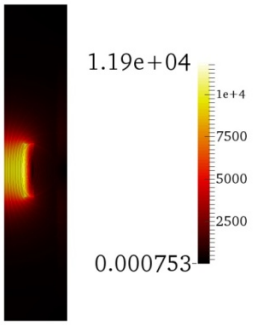

Fig. 5. Magnetic field intensity H (A/m) and field lines in a meridian plane (symmetry axis on the left) in the ferrofluid case.

The Kelvin force, generated by the magnetic field of Fig. 5, impacts the system dynamics. In this case, the velocity field does not reach a static state, as shown in Fig. 6a. The kinetic energy, after an initial transitory regime, reaches a plateau and then switches (between 8000 and 9000 s) to an oscillating

state. Further computations show that the oscillations of the kinetic energy survive after $t = 10000$ s. The temperature field reaches an almost static state, oscillations due to the changes in the velocity field being very small, in the time needed for vegetable oil (Fig. 6b). The cooling performance of ferrofluid can be assessed since the coil temperature is stable.

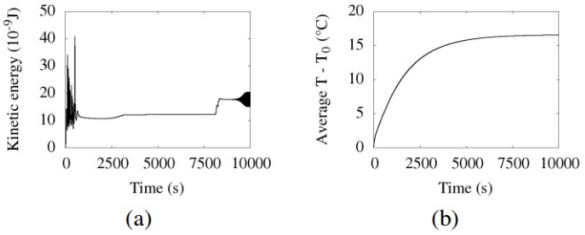

Fig. 6. Time evolution of the kinetic energy (a) and the spatial quadratic mean of the temperature increment $T - T_0$ in the ferrofluid case.

The flow pattern is transformed because of the Kelvin force. In the pure vegetable oil case (Fig. 7a), a natural convection cell appears at the top of the coil. The fluid flows up along the coil while heating and then down along the tank while cooling. In the ferrofluid case (Fig. 7b), a strong upward flow appears at the symmetry axis and leads to an additional convection cell that cools down the coil.

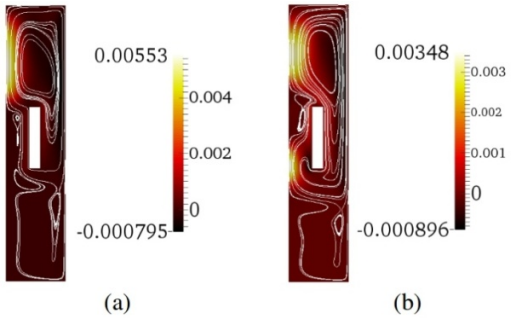

Fig. 7. Axial velocity u_z (m/s) and streamlines in a meridian plane (symmetry axis on the left) at $t = 10000$ s for regular oil (a) and ferrofluid (b).

The magnetoconvection improves the heat removal in the ferrofluid system. The temperature increment $T - T_0$ in the coil goes from 37.3 °C with regular oil to 33.8 °C with ferrofluid, see Fig. 8. Thanks to the nanoparticles, the increase of temperature in the coil is reduced by about 9.4 %.

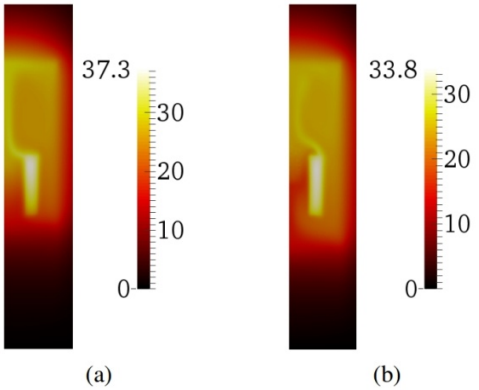

Fig. 8. Temperature increment $T - T_0$ (°C) in a meridian plane (symmetry axis on the left) at $t = 10000$ s for regular oil (a) and ferrofluid (b).

V. Conclusion

A mathematical model has been developed to study transformer cooling with ferrofluid on an immersed coil case. The action of the magnetic field on the fluid is modelled by the Kelvin force while the magnetization of the ferrofluid follows the Langevin's law for paramagnetism.

Numerical simulations based on an experimental setup are consistent with the temperature measured in the case of regular oil cooling. Numerical experiments show an improvement of the heat removal when regular oil is replaced by ferrofluid, the temperature rise in the coil being reduced by 9.4 % due to magnetoconvection.

Further developments will include a model taking into account the modification of the fluid properties with nanoparticles and the comparison with ferrofluid experimental results.

Acknowledgement

This work is supported by the Labex LaSIPS (Nano-in-Oil Grant). Code's development and simulations were performed with HPC resources from GENCI-IDRIS (Grant 2016-0254) and TAMU.

References

[1] J. L. Neuringer, and R. E. Rosensweig, "Ferrohydrodynamics," *The Physics of Fluids*, vol. 7, no. 12, pp. 1927-1937, Dec. 1964.

[2] S. Odenbach, "Magnetoviscous Effects in Ferrofluids," *Lecture Notes in Physics Monographs*, vol. 71, Springer, 2002.

[3] G.-Y. Jeong, S. P. Jang, H.-Y. Lee, J.-C. Lee, S. Choi, and S.-H. Lee, "Magnetic-Thermal-Fluidic Analysis for Cooling Performance of Magnetic Nanofluids Comparing With Transformer Oil and Air by Using Fully Coupled Finite Element Method," *IEEE Trans. Magn.*, vol. 49, no. 5, pp. 1865-1868, May 2013.

[4] L. Pîslaru-Dănescu, A. M. Morega, G. Telipan, M. Morega, J. B. Dumitru, and V. Marinescu, "Magnetic Nanofluid Applications in Electrical Engineering," *IEEE Trans. Magn.*, vol. 49, no. 11, pp. 5489-5497, Nov. 2013.

[5] J. Patel, K. Parekh, R. V. Upahyay, "Prevention of hot spot temperature in a distribution transformer using magnetic fluid as a coolant," *International Journal of Thermal Sciences*, vol. 103, pp. 35-40, 2016.

[6] J.-L. Guermond, R. Laguerre, J. Léorat, C. Nore, "Nonlinear magnetohydrodynamics in axisymmetric heterogeneous domains using a Fourier/finite element technique and an interior penalty method," *Journal of Computational Physics*, vol. 228, pp. 2739-2757, 2009.

[7] R. E. Rosensweig, "Magnetic Fluids," *Annual Review of Fluid Mechanics*, vol. 19, pp. 437-63, 1987.

[8] N. Puigmal, A. Nait Djoudi, E. Berthelot, R. Zanella, X. Mininger, "Etudes numériques et expérimentales du refroidissement par bain d'huile d'un système électromagnétique," submitted to NUMELEC 2017 conference.

[9] W. T. Perrins, D. R. McKenzie, R. C. McPhedran, "Transport properties of regular arrays of cylinders," *Proc. R. Soc. Lond. A*, vol. 369, pp. 207-225, 1979

[10] A. Bonito, J.-L. Guermond, F. Luddens, "Regularity of the Maxwell equations in heterogeneous media and Lipshitz domains," *Journal of Math. Analysis and Applications*, vol. 408, no. 2, pp. 498-512, 2013

[11] C. Nore, H. Zaidi, F. Bouillault, A. Bossavit, J.-L. Guermond, "Approximation of the time-dependant induction equation with advection using Whitney elements: Application to dynamo action," *COMPEL*, vol. 35, no. 1, pp. 326-338, 2016.

[12] A. Giesecke, C. Nore, F. Stefani, G. Gerbeth, J. Léorat, W. Herreman, F. Luddens, J.-L. Guermond, "Influence of high-permeability discs in an axisymmetric model of the Cadarache dynamo experiment," *New Journal of Physics*, vol. 14, no. 5, pp. 053005, 2012.

[13] M. Wanschura., H. C. Kuhlmann, H. J. Rath, "Three-dimensional instability of axisymmetric buoyant convection in cylinders heated from below," *J. Fluid Mech.*, vol. 326, pp. 399–415, 1996.